Molecular Cloning and Expression Profiling of Minus-C Odorant Binding Proteins from *Apocheima cinerarius* (Lepidoptera: Geometridae)[1]

Long Chen, Shengjie Zhu, Hui Lu, Lang Qiao, Yaxian Hao, and Shuiyuan Hao[2]

Hetao Area Green Agricultural Product Safety Production and Early Warning Control Laboratory, Hetao College, Bayannur, Inner Mongolia, China

J. Entomol. Sci. 59(4): 488–505 (October 2024)
DOI: 10.18474/JES23-86

Abstract Based on transcriptome data of adults and pupae, 3 Minus-C *OBPs* (odorant binding proteins) genes were cloned and analyzed in various tissues (including head, thorax, abdomen, legs of female and male adults, and wings of males) of *Apocheima cinerarius* Erschoff (Lepidoptera: Geometridae). Expression patterns were examined across the developmental stages of egg, larva (1st–5th instars), pupa (non-diapause and diapause), and adults. The qRT-PCR results revealed a significant up-regulation of *OBP8* in 3rd and 4th larval instars, with the highest expression level observed in 4th-instar larvae. *OBP14* exhibited higher expression levels in diapausing pupal and adult stages, with highest levels in the female adult. Conversely, *OBP18* displayed highest expression in the non-diapausing pupae, while exhibiting extremely low expression levels among other stages. The tissue expression profile revealed a gradual increase in the expression of *OBP14*, with highest levels in the male legs, whereas the expression pattern of *OBP18* exhibited an inverse trend with maximum expression observed in the male head (including antennae). *OBP8* exhibited high expression levels in the abdomen of the female adult, while *OBP14* showed high expression in the legs of the male adult. Additionally, *OBP18* displayed high expression in the female head. These findings suggest the crucial role played by *OBP* genes in both olfactory and non-olfactory tissues of *A. cinerarius*. The results provide a fundamental basis for further investigation into the recognition of odorant binding in *A. cinerarius*.

Key Words *Apocheima cinerarius*, odorant binding proteins, gene cloning, qRT-PCR, olfactory recognition

Apocheima cinerarius Erschoff (Lepidoptera: Geometridae) is primarily distributed in Northern China, Southeast Russia, and Central Asia (Hu et al. 2001, Liu et al. 2014) and is a pest of poplar (*Populus bonatii* Levl), willow (*Salix matsudana* Koidz), locust (*Sophora japonica* L.), mulberry (*Morus alba* L.), and other tree species, as well as Korshinsk pea shrub (*Caragana korshinskii* Kom) and Russian olive (*Elaeagnus angustifolia* L.). Larvae are foliage feeders with continuous feeding leading to host plant death and eventual destruction of the forest landscape (Furniss and Carolin 2015, Millar et al. 1990).

Of special concern is its impact on *C. korshinskii* which is highly suitable for mitigating wind erosion in the central and western regions of Inner Mongolia. These

[1]Received 18 November 2023; accepted for publication 4 February 2024.
[2]Corresponding author (email: 451298669@qq.com).

areas suffer from severe soil desertification, resulting in low productivity and a fragile ecological environment. In recent years, infestations of *A. cinerarius* have significantly impacted the livelihoods of farmers and herdsmen, exacerbating destruction of an already vulnerable grassland ecosystem. Control of the pest in such areas is not cost effective and presents additional environmental problems. Ecologically friendly and cost-effective methods for the prevention and control of *A. cinerarius* must be immediately addressed.

The pest impact of *A. cinerarius* is closely associated with specific physiological behaviors, including aggregation, migration, feeding, robust reproductive capacity, and evasion of natural enemies. These behaviors are intricately linked to its highly evolved olfactory sensory system.

Olfaction is essential for the survival and reproduction of insects. It is involved in insect feeding, mate finding, oviposition site selection, and the completion of life activities such as individual and group communication (Su et al. 2009). It includes odorant binding proteins (OBPs), chemosensory proteins (CSPs), odorant receptors (ORs), ionotropic receptors (IRs), sensory neuron membrane proteins (SNMPs), and odorant degradation enzymes (ODEs). These proteins are highly coordinated to complete the process of recognition and assimilation of environmental information (Yang et al. 2019).

The process of recognition of the external environment initiates with interactions of OBPs and chemical substances present in the surrounding environment (Feng and Prestwich 1997, Liu et al. 2015; Swarup et al. 2011,). Based on conserved cysteine residues in their amino acid sequences, OBPs can be categorized into Classical OBP, Min, and OBP (Du Yali et al. 2020). At present, more than 150 OBPs have been identified from 35 species of 13 lepidopteran families (Zhou et al. 2010). Studies with many insects, such as *Anoplophora glabripennis* Motschulsky (Hu et al. 2016; Wang et al. 2017, 2019), *Ectropis obliqua* Warren (Ma 2016, Yan et al. 2021), and *Cydia pomonella* (L.) (Tian 2016), have been conducted on the types, functions, and olfactory mechanisms of olfactory-related proteins. Many have shown that antennae are an important part of OBP expression, but OBPs are also expressed in other tissues such as the head, thorax, and abdomen (Zhang et al. 2017). Expression of OBPs related to gender and developmental activities also vary.

Relevant studies have indicated that OBPs play roles in recognition, but they may also serve non-olfactory functions. For example, approximately one-half of the OBP transcripts identified in *Sesamia inferens* Walker are also weakly expressed in non-chemoreception organization (thorax and abdomen), suggesting that these OBPs may possess other functions (Zhang et al. 2013). Among the 38 *SlitOBP* transcripts of *Spodoptera litura* F., 17 exhibit unique or predominant expression in male and female antennae and, thus, potential involvement in chemoreception (Gu et al. 2015). The expression of *litOBP11* in larval antennae at higher levels than that in adult antennae suggests potential involvement in the olfactory process of larvae (Luo et al. 2021). The antennae of *Eogystia hippophaecolus* Hua, Chou, Fang & Chen exhibit the highest expression levels of most OBPs, with *OBP6* showing a male reproductive bias expression, identification, and combination of pheromones for mating. In addition, *OBP1* has the highest expression level in the tarsus, which may have the function of identifying host plant volatiles (Hu et al. 2016). The OBPs genes of *Pieris rapae* L. showed gender-biased expression. *PrapOBP1, 2, 4* and *13* were expressed in the male antennae, while *PrapOBP7* and *PrapOBP10* were expressed in female antennae (Li et al. 2020).

The objectives of this study were to (1) clone 3 Minus-C OBPs through RT-PCR, utilizing transcriptome data from both adults and pupae of *A. cinerarius*, (2) identify their sequence signature, physicochemical properties, and bioinformatics as well as the distribution patterns of *AcinOBP8*, *AcinOBP14*, and *AcinOBP18* across different developmental stages and tissues of *A. cinerarius* using qRT-PCR, and (3) identify efficient and environmentally friendly target sites for management of this pest.

Materials and Methods

Experimental design. In the winter of 2021, *A. cinerarius* overwintering pupae were collected and cultured under controlled laboratory conditions (22 ± 1°C, 18:6 h L:D photo regime, 55–59% relative humidity). Upon emergence, male and female adults were paired and reared on *C. korshinskii*. After oviposition, they were collected and divided into 2 groups. One group was quick-frozen in liquid nitrogen for future use, while the other group underwent further rearing. Larvae were continuously reared using *C. korshinskii* until reaching the pupal stage. The experimental treatments were: (1) developmental stages of eggs, larvae (1–5 instars) (2 days after molting), pupae (diapause and non-diapause), and adults; and (2) tissues from head (including antennae), thorax, abdomen, legs of male and female adults, and wings of male adults.

The experiment included 3 biological replicates, with each replicate containing 30 eggs, 30 first-instar larvae, 20 second-instar larvae, 3rd–5th instar larva, pupae, and male and female adults ($n = 3$), 30 heads, 5 thoraxes and 5 abdomens. Additionally, 50 leg samples were taken for each type of the leg (e.g., foreleg, midleg, and hindleg), and 20 male wing samples. The samples were quick-frozen in liquid nitrogen and stored at a temperature of −80°C.

RNA extraction. The RNA extraction kit, reverse transcription kit for cDNA synthesis of strand 1, PCR reaction MIX, and pMD19-T connection vector were procured from Dalian Bao Biological Technology Company (Dalian, Liaoning, China). The 5α competent cells were obtained from Beijing Tiangen Biochemical Technology Company (Changping District, Beijing, China). The GoTaq® qPCR Master Mix (2×) was purchased from Promega Corp (Madison, WI).

Total RNA extraction and synthesis of the first strand cDNA were accomplished by placing insects in a pre-cooled mortar that had been sterilized at high temperature and cooled with liquid nitrogen. The RNA extraction procedure followed the instructions of the TaKaRa RNA extraction kit. The quality and concentration of RNA extraction were detected using 1.0% agarose gel electrophoresis and NanoPhotometer-N50 ultra microspectrophotometer. Subsequently, the first strand of cDNA was synthesized through reverse transcription following successful evaluation.

Cloning. Based on the *OBP* genes identified from the transcriptome data of adults and pupae of *A. cinerarius* in our laboratory, 3 Minus-C *OBPs* were identified for experiments, and primers were designed using Primer Premier 5.0 software (Table 1). The protein coding region of the *OBP* genes was amplified using the synthesized cDNA as the amplification template. The PCR reaction system (25 μL) consisted of 1 μL cDNA amplification template, 1 μL forward and 1 μL reverse primers, 12.5 μL PCR Mix, and RNase-free water to fill the remaining volume. The PCR reaction procedure included pre-denaturation at 94°C for 3 min, denaturation

Table 1. Primers used for real time fluorescence quantitative PCR and gene cloning reaction.

Gene	Primer sequences (5'-3')	Purpose
*AcinOBP*8	F: CTGAAGACGTCAGACGTGTCTCG R: GATGAACGGAGATCAAAGGATAGAA	Gene cloning
*AcinOBP*14	F: CAGGACCGGATATGACGACTAGACTACT R: GGCCATCTATTGGTGAAAACCATGC	
*AcinOBP*18	F: ATGAAGACTTTGCTGGTTCTAACCG R: TGTTAGAATGCATCAGCTGTATCCAC	
*AcinOBP*8	F: AATGTGCTGGCAGTGAATCC R: TTCTACGGCCGTATTCCCTC	qRT-PCR
*AcinOBP*14	F: GGCTGAGAAGGCGATGTTTC R: CGTCTTTCCCCACAACCTTG	
*AcinOBP*18	F: ACTGAGAACGAGCCACTGAA R: GTCTGTTGGGGCGTATTTCC	
Actin	F: CGACATCCGTAAGGACCTGT R: TTCGAGATCCACATCTGCTG	

at 94°C for 30 s, annealing at 62°C for *OBP8*, 66°C for *OBP14*, 62°C for *OBP18*, extension at 72°C for 1 min, repeated for a total of 30 cycles, filled and extended at 72°C for 10 min, and finally stored at 4°C. The size of the destination strip was adjusted to match the desired specifications, was connected to the pMD19-T vector, and transformed into DH5α *E. coli* using 1% agarose gel electrophoresis detection. Subsequently, the white-blue plaque selection was conducted. After culturing at 37°C, 3 randomly selected positive colonies of the expected size were sent to Biotechnology Limited Company of Shanghai for sequencing.

Bioinformatics analysis. The ORF Finder (https://www.ncbi.nlm.nih.gov/orffinder) of the NCBI online website was used to predict the coding protein region of the OBP gene of *A. cinerarius*. The DNAMAN 6.0 (Lynnon Biosoft, Quebec, Canada) software was used to analyze the sequence identity of the OBP gene between the selected other insects and the *A. cinerarius*. SignalIP5 (http://www.cbs.dtu.dk/services/SignalP/ online prediction tool) was used to predict the N-terminal signal peptide of odorant binding protein of *A. cinerarius*. ExPASy-ProtParam tool (http://web.expasy.org/protparam/ software) was used to predict the physicochemical properties of the OBP gene of *A. cinerarius*. The phylogenetic tree was constructed by MEGA6.0 software, and the neighbor-joining (NJ) and p-distance were used to repeat the process 1,000 times.

Expression profile. Based on the cloned OBPs gene sequence, primers were designed using the Primer3 online website (Table 1). Amplification length was between 80–250 bp, and the optimal dilution of cDNA template was selected, with Actin as the reference gene. qRT-PCR was performed to amplify the 3 OBP target genes and reference genes. The reaction system consisted of 20 μL: template cDNA (2 μL), 1 μL forward and 1 μL reverse primers (0.4 μL each), GoTaq® qPCR

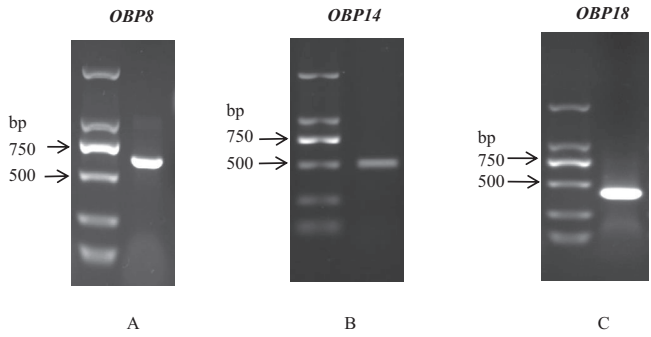

Fig. 1. Cloning of full length CDS of *AcinOBP* in *A. cinerarius.*

Master Mix (10 μL), and Nuclease-Free Water (7.2 μL). The reaction procedure followed the instructions provided by GoTaq® qPCR Master Mix. Based on the expression level of OBPs in male head, the obtained data were analyzed by $2^{-\Delta\Delta Ct}$ (Livak and Schmittgen 2001). The expression of *AcinOBP* in various tissues and developmental stages was quantified. Each tissue and stage had 3 biological replicates and 3 technical replicates.

Data statistics and analysis. The data analysis was performed using SPSS 20.0 software. Tukey's honestly significant difference (hsd) was employed to analyze the relative expression of 3 *OBPs* genes across different tissues and developmental stages. The Least Significant Difference (LSD) T test was used to assess the gene expression within the same tissue but across gender. GraphPad Prism 7.0 software was utilized for generating histograms, presenting mean ± SD, with statistical significance set at $P < 0.05$.

Results

Cloning and sequence analysis of OBPs. According to the transcriptome database, we designed primers targeting sequences of 3 OBPs for amplification: 662 bp, 503 bp, and 441 bp (Fig. 1A–C). By comparing the sequences of the 3 OBPs genes with the transcriptome data, we found that the sequence information remained consistent. We assigned them as *AcinOBP8*, *AcinOBP14*, and *AcinOBP18*. The corresponding GenBank accession numbers are MT999864, MT999870, and MT999874 (Table 2).

The full-length coding sequences (CDS) of *AcinOBP8*, *AcinOBP14*, and *AcinOBP18* were 402 bp, 462 bp, and 444 bp in length, respectively (Fig. 2A–C). These CDS encoded proteins consisted of 147, 153, and 133 amino acids. The predicted molecular weights for these proteins were determined to be approximately 16.70 kDa, 16.66 kDa, and 15.02 kDa with isoelectric points of approximately 5.93, 8.40, 9.46, respectively. Furthermore, the presence of signal peptides was detected within the aforementioned genes.

Physicochemical properties. The physicochemical properties of the 3 Minus-C OBPs were predicted using the ExPASy-ProtParam software (Table 3). Amino acid residues for the 3 Minus-C genes were 147, 153, and 133, and molecular weights were determined to be 16.71, 16.66, and 15.03, respectively. Additionally,

Table 2. Statistical table of basic information of OBPs gene in *A. cinerarius*.

Genes	GenBank accession No.	Nucleotide length/bp	Signal peptide	CDS integrity	Amino acid length/ aa	BLAST annotation	BlastP test and verify		
							GenBank accession No. of homogenous protein	E-value	Identity/%
*AcinOBP*8	MT999864	402 bp	1–21	Yes	147	*Operophtera brumata*	KOB71255.1	6e-30	44.44%
*AcinOBP*14	MT999870	462 bp	1–20	Yes	153	*Ectropis grisescens*	UWK22043.1	9e-62	89.32%
*AcinOBP*18	MT999874	444 bp	1–16	Yes	133	*Ectropis obliqua*	ALS03864.1	2e-83	90.98%

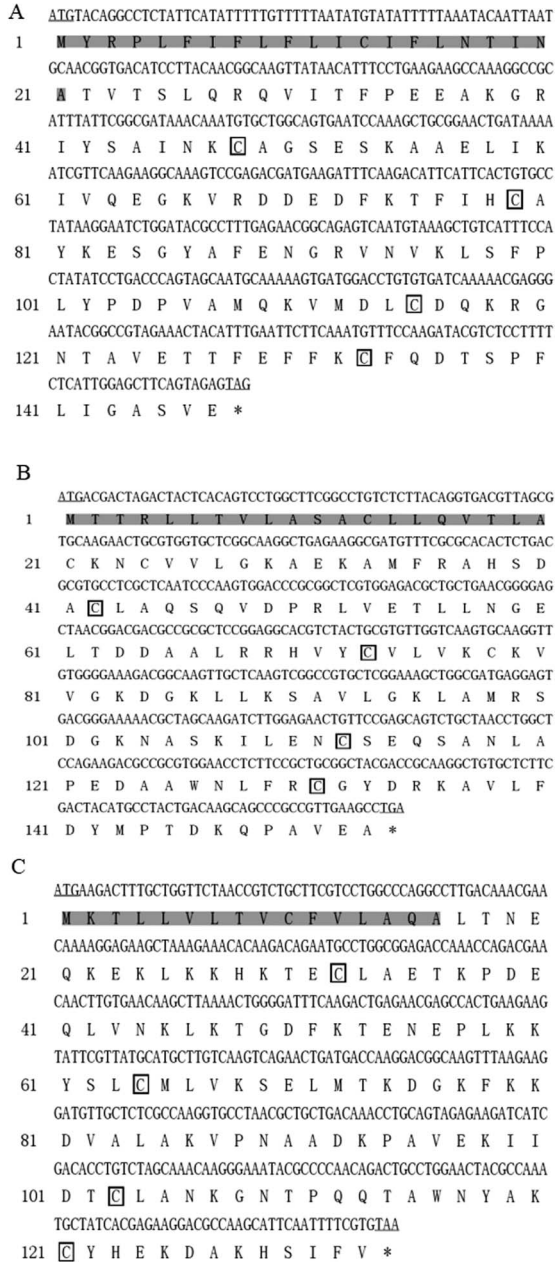

Fig. 2. Nucleotide and encoded deduced amino acid sequence of AcinOBP8 (A), AcinOBP14 (B) and AcinOBP18 (C) in *A. cinerarius.* The shadow part is the signal peptide. Boxes: four cysteines.

Table 3. Physicochemical properties of OBPs protein of *A. cinerarius*.

Gene	Amino acids	Molecular weight/kD	Isoelectric point	Negatively charged residues	Positively charged residues	Instability index	Aliphatic index	Average Hydropathicity
AcinOBP8	147	16.71	5.87	18	17	30.67	82.93	−0.020
AcinOBP14	153	16.66	8.63	17	21	44.26	98.24	0.016
AcinOBP18	133	15.03	9.12	17	24	25.88	81.43	−0.523

their predicted theoretical iso-electric points were found to be at pH values of 5.87, 8.63, and 9.12, respectively. The results demonstrated that *AcinOBP8* was classified as an acidic protein, whereas *AcinOBP14* and *AcinOBP18* were categorized as alkaline proteins. The net charge of *AcinOBP8* was characterized by a greater number of negative charge residues compared to positive charge residues, whereas the net charge of *AcinOBP14* and *AcinOBP18* exhibited a reversed trend with fewer negative charge residues than positive charge residues. The instability coefficients of *AcinOBP8* and *AcinOBP18* were <40, while the instability coefficient of *AcinOBP14* >40. This suggests that *AcinOBP8* and *AcinOBP18* represent stable proteins, in contrast to *AcinOBP14*, which displays characteristics of an unstable protein. The protein's thermal stability was indicated by the Aliphatic index, and the results demonstrated that all OBPs were thermally stable proteins. *AcinOBP8* and *AcinOBP14* had a total average hydrophobicity of -0.020 and 0.016, respectively, indicating that these gene proteins were amphoteric proteins. On the other hand, *AcinOBP18* had a total average hydrophobicity of -0.523, suggesting that this gene was hydrophilic (where positive values indicate hydrophobicity while negative values indicate hydrophilicity; the range of -0.5 to 0.5 represents amphoteric proteins).

Sequence alignment and phylogenetic relationship analysis. By comparing the amino acid sequences of the 3 *OBPs* of the *A. cinerarius* with those of other Lepidoptera (Figs. 2, 3), it was observed that *AcinOBP8* exhibited the highest sequence similarity to *Dendrolimus kikuchii* Matsumura OBP (32.43%), while displaying lower similarities to *Operophtera brumata* L., *Semiothisa cinerearia* Bremer & Grey, and *E. obliqua* (16.99%, 13.12%, and 8.84%, respectively). *AcinOBP14* demonstrated the highest sequence consistency with *E. obliqua* OBP (72.90%), followed by *Streltzoviella insularis* Staudinger (59.75%), *E. obliqua* (21.42%), and *O. brumata* (11.42%). *AcinOBP18* displayed the highest sequence consistency with *E. obliqua* OBP16 (90.98%), followed by *Galleria mellonella* L. OBP56a (85.71%), which exceeded 13.10% for *S. cinerearia* and 8.63% for *O. brumata*.

The phylogenetic analysis revealed that *AcinOBP8*, *AcinOBP14*, and *AcinOBP18* formed a distinct clade (Fig. 4). Specifically, *AcinOBP8* and *ObruOBP* were grouped together, while *AcinOBP14* and *ScinOBP* clustered in another branch. Furthermore, *AcinOBP18* showed close genetic relationship with *GmelOBP56a* and *EoblOBP16*. The results showed that *AcinOBP8*, *AcinOBP14*, and *AcinOBP18* were closely related to the OBPs of *O. brumata*, *S. cinerearia*, and *E. obliqua*, respectively. In addition, *AcinOBP18* was also closely related to the OBP of *G. mellonella*.

Expression profiles at different developmental stages. The expression patterns of the 3 *OBPs* in *A. cinerarium* at different developmental stages are depicted in Fig. 5 (*OBP14* was not expressed in the 4th-instar larvae). *OBP8* exhibited an increasing trend initially, reaching its peak during the 4th instar, followed by a decrease. The expression levels were 69.10 and 29.97 times higher than the control (egg stage) for the 3rd and 4th instars, respectively, with a significant difference ($P<0.05$). No significant differences were found among other developmental periods.

The expression of *OBP14* showed a gradual increase, reaching the maximum in males, followed by diapausing pupal and adult female stages, which were 240.45, 121.69, and 51.85 times that of the control, respectively, and were significantly different ($P<0.05$). There was no significant difference in expression levels in other

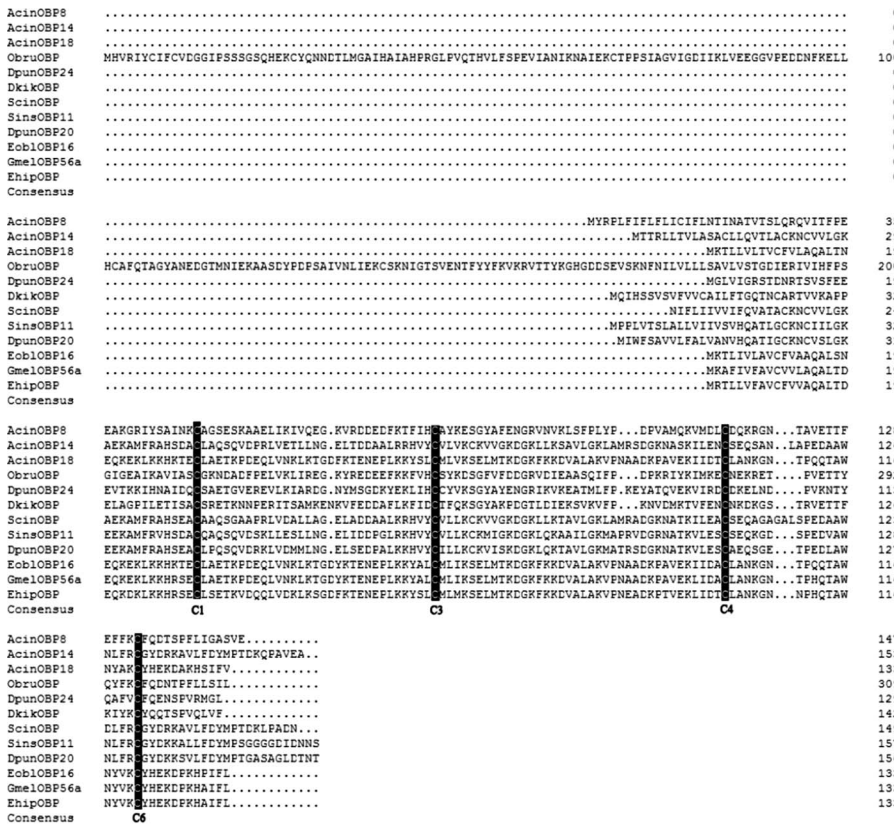

Fig. 3. Multiple amino acid sequence alignment of OBPs from *A. cinerarius* and other insects.

Note: Source species of OBPs proteins and their GenBank accession numbers. *Apocheima cinerarius* (AcinOBP8: MT999864; AcinOBP14: MT999870; AcinOBP18: MT999874); *Operophtera brumata* (ObruOBP: KOB71255.1); *Dendrolimus punctatus* (DpunOBP24: ARO70183.1); *Dendrolimus kikuchii* (DkikOBP: All01002.1); *Semiothisa cinerearia* (ScinOBP: QRF70927.1); *Streltzoviella insularis* (SinOBP11: QLI62014.1); *Dendrolimus punctatus* (DpunOBP20: ARO70179.1); *Ectropis obliqua* (EobliquaOBP16: ALS03864.1); *Galleria mellonella* (GmelOBP56a: XP_026763748.1); *Eogystia hippophaecolus* (EhipOBP: AOG12864.1).

periods of development. The expression of *OBP18* was mainly concentrated in non-diapause pupae, which were 84.54 times that of the control and were significantly different ($P < 0.05$). The expression level of *OBP18* was extremely low in other periods, with no obvious difference.

Tissue expression profile. The qPCR results revealed the expression of 3 *OBPs* in all examined tissues of *A. cinerarius* (Fig. 6). Notably, distinct expression patterns were observed for these genes across different tissues in male and

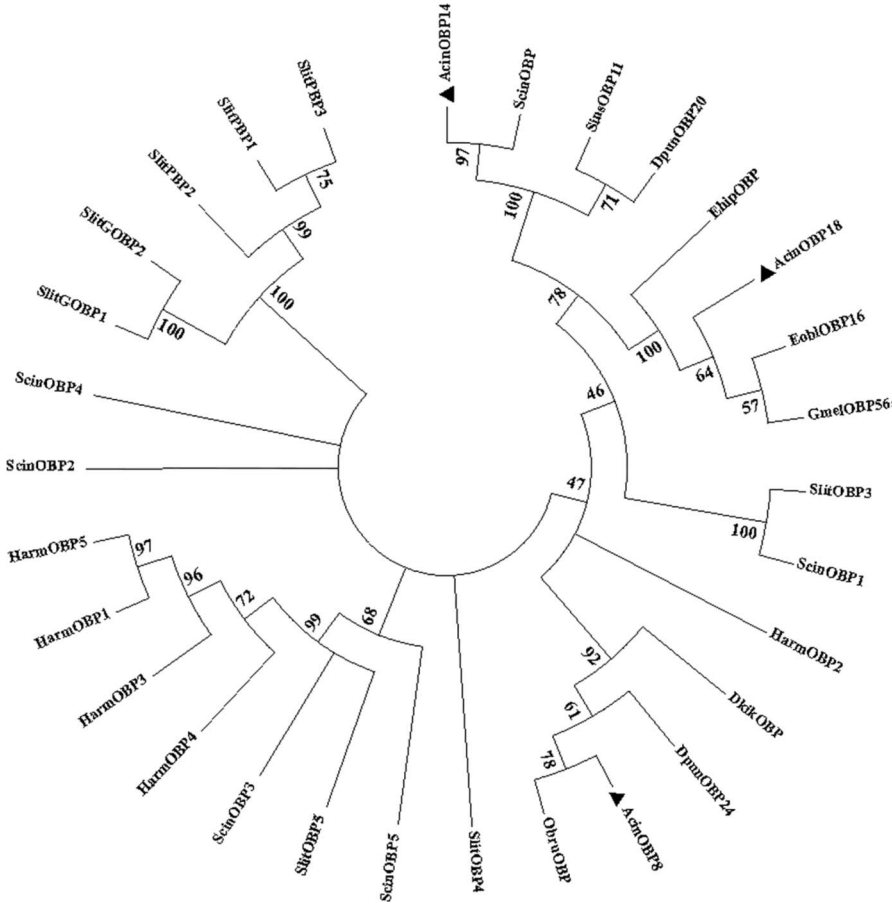

Fig. 4. Phylogenetic tree based on amino acid sequence of OBPs from *A. cinerarium* and other insects.

Note: The tree was constructed by MEGA 6.0 using the Neighbor-Joining (NJ) method, the OBPs protein of *A. cinerarium* was marked with filled circle. Source species of OBPs proteins and their GenBank accession numbers. *Apocheima cinerarius* (AcinOBP8: MT999864; AcinOBP14: MT999870; AcinOBP18: MT999874); *Operophtera brumata* (ObruOBP: KOB71255.1); *Dendrolimus punctatus* (DpunOBP24: ARO70183.1); *Dendrolimus kikuchii* (DkikOBP: AII01002.1); *Semiothisa cinerearia* (ScinOBP: QRF70927.1); *Streltzoviella insularis* (SinsOBP11: QLI62014.1); *Dendrolimus punctatus* (DpunOBP20: ARO70179.1); *Ectropis obliqua* (EoblOBP16: ALS03864.1); *Galleria mellonella* (GmelOBP56a: XP_026763748.1); *Eogystia hippophaecolus* (EhipOBP: AOG12864.1); *Dendrolimus punctatus* (*DpunOBP24*; ARO70183.1); *Spodoptera litura* (SlitPBP1: AIS72935.1; SlitPBP2:QYF65652.1; SlitPBP3: AIS72934.1; SlitGOBP1: XP_022816701.1;SlitGOBP2: AKI87961.1;SlitOBP3: XP_022827633.1; SlitOBP4: XP_022832058.1;

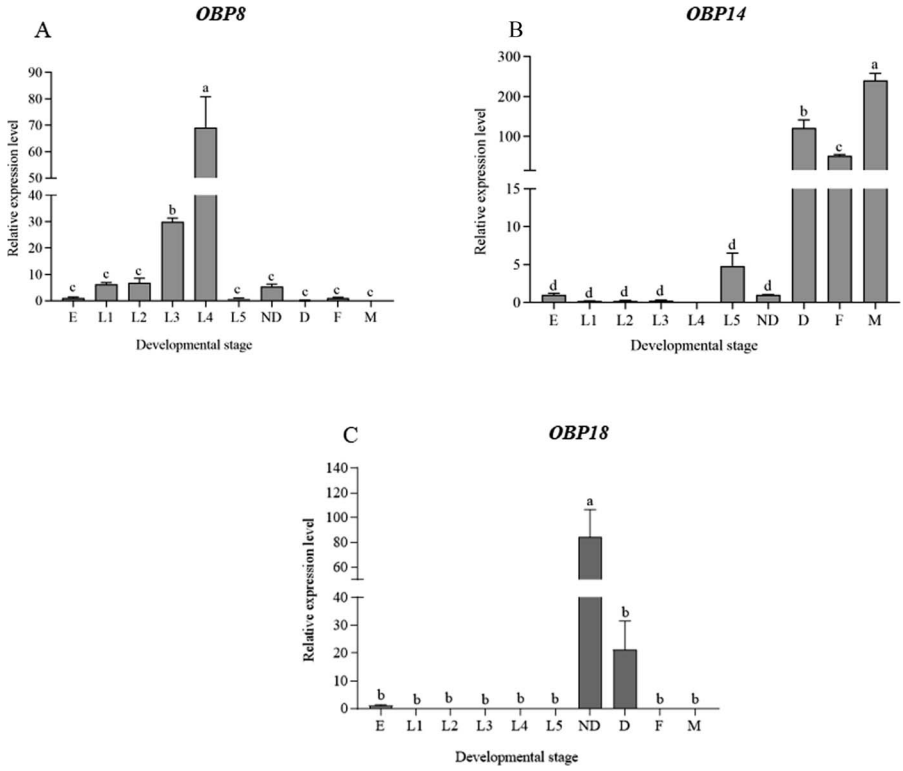

Fig. 5. Expression levels of *AcinOBP* in different developmental stages of *A. cinerarius.*

female adults of *A. cinerarius*. Specifically, the expression level of *OBP8* exhibited a gradual increase followed by a decrease in the head, thorax, and abdomen of both male and female adults. Among females, the highest expression level was detected in the abdomen, reaching 13.12 times higher than that of the control group. Conversely, lower expression levels were observed in the legs and wings of males, ranging from only 0.08 to 0.58 times than that of the control.

The *OBP8* expression showed significant differences only in the abdomen and legs of adult males and females, while no significant differences were observed in other body parts. The expression level of the *OBP14* was low in each tissue of female *A. cinerarius*, with no significant difference detected. In male insects, except

←

SlitOBP5: AKI87966.1); *Helicoverpa armigera* (HarmOBP1: AEB54580.1; HarmOBP2: AEB54586.1; HarmOBP3: AEB54582.1; HarmOBP4: AEB54584.1; HarmOBP5: AEB54581.1); *Semiothisa cinerearia* (ScinOBP1: QRF70921.1; ScinOBP2: QRF70922.1; ScinOBP3: QRF70923.1 ScinOBP4: QRF70924.1; ScinOBP5:QRF70925.1).

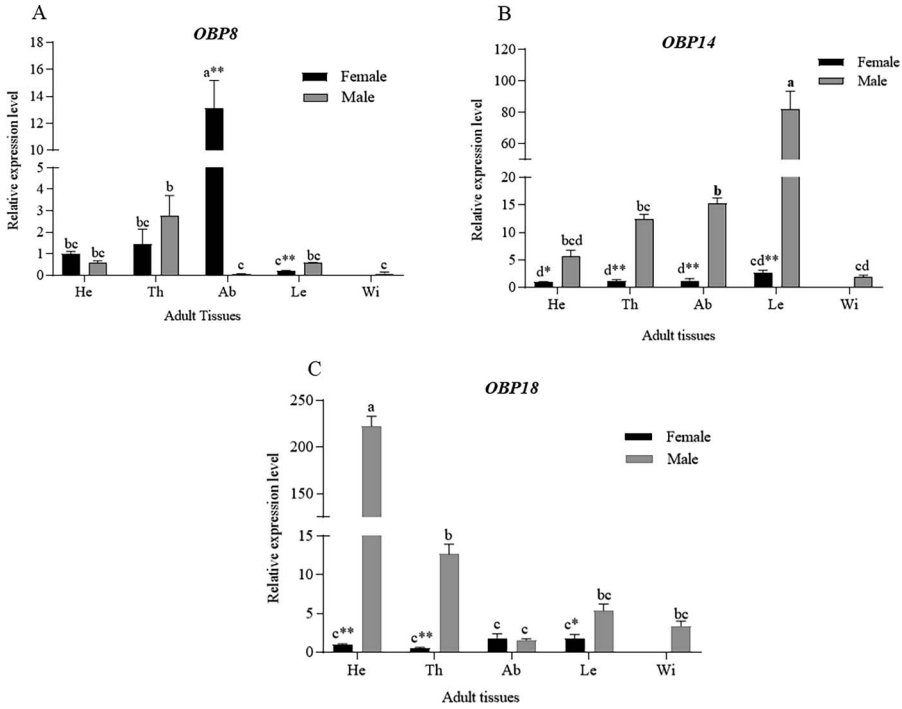

Fig. 6. Expression levels of *AcinOBP* in different tissues of *A. cinerarius* adults.

for wings, there was a gradual increase in the expression levels across different tissues. Specifically, the expression levels in legs, abdomen, thorax, and head were 81.97 times, 15.27, 12.39, and 5.64 times greater than that of the control group, respectively. Moreover, compared to females, males exhibited significantly higher expression levels of *OBP14* in their heads, thorax, abdomens, and legs ($P < 0.01$). The expression pattern of *OBP18* in *A. cinerarius* was the same as that of *OBP14*, the expression level in each tissue was low and there was no significant difference, while the expression level in male insects was opposite to that of *OBP14*. It showed a gradual downward trend, and the expression levels in the head and thorax of males were 222.52 and 12.67 times that of the control, respectively. The expression levels in male and female legs were significantly different, while in the head and abdomen reached a significant difference ($P < 0.01$).

Discussion

Odorant binding protein (OBP) is a low molecular weight acidic soluble protein that is widely distributed in the lymph of insect antennae. It typically has a relative molecular weight ranging from 15 to 20 kD and is characterized by the presence of a signal peptide at its N-terminus, consisting of approximately 20 amino acids

(Paula et al. 2016, Wang et al. 2022). Generally, OBP contains 6 conserved cysteines, while Minus-C OBPs lack 2 of these conserved cysteines (Gao et al. 2023).

In this study, 3 OBPs gene, namely *AcinOBP8*, *AcinOBP14*, and *AcinOBP18*, were identified for the first time based on transcriptome data from *A. cinerarius* adults and pupae. Notably, these proteins exhibited a lack of the second and fifth cysteines, suggesting their classification as Minus-C OBPs.

Furthermore, the presence of signal peptides in the 3 OBPs genes examined in this study suggests their classification as secretory proteins. However, it should be noted that certain OBP proteins such as *SfruOBP3,31,35,41,55-56,59-61*, and *Spodoptera frugiperda SfruOBP1,7,9,14,17-18,20,23-24* and *26-27* (Jia et al. 2023) in *A. glabripennis* lack a signal peptide at the N-terminus. Conversely, *MaltOBP1* from *Monochamus alternatus* Hope (Zhang et al. 2020), *AglaOBP* (Li et al. 2018), and *YsigOBP1-YsigOBP10* from *Yemma signatus* Hsiao (Song et al. 2021) exhibit signal peptides at their N-terminus. These findings indicate that the presence or absence of signal peptides does not serve as an identifying feature for insect odorant binding proteins.

In this study, the identity of *AcinOBP8* with *O. brumata* and *S. cmerearia* was lower than that of *D. kikuchii* (32.43%), with the lowest identity being only 8.84% for *E. obliqua*. On the other hand, *AcinOBP14* showed a higher identity with the OBP sequence of *S. cmerearia* at 72.90%, while its similarity to *E. obliqua* was lower. Finally, *AcinOBP18* had the highest identity with OBP16 sequence of *E. obliqua* at 90.98%, but its similarities to both *S. cmerearia* and *O. brumata* were only 13.10% and 8.63%, respectively. Similar findings were also observed in other insects. For instance, *HtheOBP3* exhibited the highest homology with *PmicOBP4*; however, their sequence similarity was only 55.56% (Zhang et al. 2023). Conversely, the sequence identity between *Bactrocera minax* Enderlein *BminOBP25* and *Dacus dorsalis* Hendel *BdorOBP* was determined to be 88% (Si et al. 2018), indicating varying degrees of differentiation among different OBPs within and across insect species.

In general, homologous sequence consistency is generally higher, however, it is important to note that two sequences with low consistency may still be considered homologous. In this study, the identity between *AcinOBP8* and the OBP sequence of *D. kikuchii* was found to be 32.43%, which is higher than that of *O. brumata* (16.99%). Nevertheless, in the phylogenetic analysis, *AcinOBP8* exhibited a closer genetic relationship to *O. brumata* despite its lower sequence identity. Similar findings were also reported in a study of *Helopeltis theivora* Waterhouse (Zhang et al. 2023).

The distribution range of OBPs in insects is widely believed to be closely associated with their functional roles, and gene expression profiling serves as a crucial approach for investigating gene function. In this study, qPCR was applied to examine the expression patterns of *OBP8* during different developmental stages and in various tissues of male and female adults. Our findings revealed that *AcinOBP8* exhibited consistent expression throughout the developmental stages, with significantly higher levels observed in the 3rd and 4th larval instars. Notably, the highest expression level was detected in 4th-instar larvae. *SzeaOBP1* and *SzeaOBP28* were expressed in both larval and adult stages of *S. zeamais*, but the expression levels differed (Tang et al. 2019). *TcasOBP7G* is expressed at all developmental

stages and is highly expressed in late larvae and late adults (Gao et al. 2023). This may be related to the feeding activity of larvae and adults, because *OBPs* are related to the dissolution of fatty acids in food (Ishida et al. 2013) and the transport of nutrients (Ribeiro et al. 2014). *AcinOBP8* exhibited high expression exclusively in the 3rd-4th instar larvae due to comparative food ingestion during the egg and adult stages of the *A. cinerarius*. The dietary intake gradually increased from the 1st- to 4th-instar larvae, reaching its peak in the 4th instar, followed by a decline after the 5th instar. In the pupal stage, no feeding occurred, thus its high expression in the 3rd-4th instar larval stage. *AcinOBP14* is highly expressed during the pupal diapause and adult stages, potentially playing a crucial role in olfactory recognition of external environmental cues for both pupae and adults. Given that *A. cinerarius* diapausing pupae experience extreme temperature variations throughout hot summers and cold winters, this OBP may aid *A. cinerarius* perception of adverse factors in their external environment.

Furthermore, the absence of *AcinOBP14* in the 4th-instar larvae may be attributed to its low expression levels, which were below the detection limit in the selected tissues and developmental stages during qPCR analysis. Additionally, among the 39 *OBPs* identified in *P. xylostella*, 12 were not detected (Cai et al. 2021). Notably, *AcinOBP18* exhibited significantly higher expression levels during non-diapause periods compared to other times ($P < 0.05$), suggesting its potential involvement in physiological processes beyond olfactory recognition.

The physiological functions of genes are usually related to their expressed tissues (Hua et al. 2012). The physiological functionality of a gene is typically associated with the tissue in which it is expressed (Hua et al. 2012). Most *OBP* genes are specifically or highly expressed in insect antennae, which is related to the involvement of *OBPs* as carriers in transporting fat-soluble odor molecules through antennal lymph (Benton et al. 2007). The expression of *OBP18* was found to be significantly up-regulated in the male head (including the antennae), as revealed by our study. In this study, a significant level of *OBP18* expression was observed in the male head. The expression levels of *AmalOBP3* and *AmalOBP8* in *Agrilus mali* Matsumura are not only highly expressed in the antennae, but also detected in the abdomen and wings (Cui et al. 2018). The expression level of *AcinOBP8* was highest in the abdomen of female insects, indicating its potential involvement in oviposition site selection or sex pheromone production. Conversely, *AcinOBP14* exhibited the highest expression level in the legs of male insects, suggesting its role in mate searching or transportation of non-volatile odorants (Jia et al. 2020). Some OBPs of *Culex pipiens* L. (Pelletier and Leal 2009), *Anopheles gambiae* Giles (Li et al. 2004), *Apis mellifera* L. (Foret and Maleszka 2006), and *Bemisia tabaci* Gennadius (Wang et al. 2017) are also highly expressed in various other parts of insects, suggesting that these OBPs may perform other physiological functions beyond their role in olfactory recognition.

The present study focused on the cloning of 3 Minus-C OBPs genes and investigated their expression profiles across various tissues, developmental stages, and gender in the *A. cinerarius*. Our findings provide information regarding the sequence, physicochemical properties, and expression pattern map of these 3 Minus-C *OBPs* in this species, thereby providing a foundation for future investigations into the functional roles of Minus-C *OBPs*.

Acknowledgments

This work was supported by the designated funding from the Inner Mongolia Natural Science Foundation (2021BS03028), the industrialization ability of flint wheat in the yellow river basin was improved (NMKJXM202201), and the Key Scientific Research Project of Hetao College (HYZZ201927).

References Cited

Benton, R., K.S. Vannice and L.B. Vosshall. 2007. An essential role for a CD36-related receptor in pheromone detection in *Drosophila*. Nature 450: 289–293.

Cai, L.J., L.S. Zheng, Y.P. Huang, W. Xu and M.S. You. 2021. Identification and characterization of odorant binding proteins in the diamondback moth, *Plutella xylostella*. Insect Sci. 28: 987–1004.

Cui, X., D. Liu, K. Sun, Y. He and X. Shi. 2018. Expression profiles and functional characterization of two odorant-binding proteins from the apple buprestid beetle *Agrilus mali* (Coleoptera: Buprestidae). J. Econ. Entomol. 111: 1420–1432.

Du, Y.L., K. Xu, H.T. Zhao, Y.L. Liu, Q.S. Niu and Y.S. Jiang. 2020. Research progress in odorant binding proteins of insects. Acta Entomol. Sinica 63(3): 365–380.

Feng, L. and G.D. Prestwich.1997. Expression and characterization of a lepidopteran general odorant binding protein. Insect Biochem. Mol. Biol. 27(5): 405–412.

Foret, S. and R. Maleszka. 2006. Function and evolution of a gene family encoding odorant binding-like proteins in a social insect, the honey bee (*Apis mellifera*). Genome Res. 16: 1404–1413.

Furniss, R.L. and V.M. Carolin. 2015. Western forest insects. USDA For. Serv., Misc. Publ. 26: 145–146.

Gao, S.S., X.Y. Zhang, J.J. Zhou, G.Y. Zhang, Y.L. Zhang, R.M. Li and K.P. Zhang. 2023. Minus-C odorant binding protein *TcasOBP7G* contributes to reproduction and defense against phytochemical in the red flour beetle, *Tribolium castaneum*. J. Asia-Pac. Entomol. 26(4): 102151.

Gu, S.H., J.J. Zhou, S. Gao, D.H. Wang, X.C. Li, Y.Y. Guo and Y.J. Zhang. 2015. Identification and comparative expression analysis of odorant binding protein genes in the tobacco cutworm *Spodoptera litura*. Sci. Rep. 5(1): 13800.

Hu, J.J., Y. Tian, Y. Han, L. Li and B. Zhang. 2001. Field evaluation of insect-resistant transgenic *Populus nigra* trees. Euphytica 121: 123–127.

Hu, P., J. Tao, M. Cui, C.L. Gao, P.F. Lu and Y.O. Luo. 2016. Antennal transcriptome analysis and expression profiles of odorant binding proteins in *Eogystia hippophaecolus* (Lepidoptera: Cossidae). BMC Genomics 17(1): 651.

Hua, J.F., S. Zhang, J.J. Cui, D.J. Wang, C.Y. Wang, J.Y. Luo and L.M. Lv.2012. Identification and binding characterization of three odorant binding proteins and one chemosensory protein from *Apolygus lucorum* (Meyer-Dur). J. Chem. Ecol. 38(9): 1163–1170.

Ishida, Y., J. Ishibashi and W.S. Leal. 2013. Fatty acid solubilizer from the oral disk of the blowfly. PLoS One 8: e51779.

Jia, C., A. Mohamed, A.M. Cattaneo, X. Huang, N.O. Keyhani, M. Gu, L. Zang and W. Zhang. 2023. Odorant-binding proteins and chemosensory proteins in *Spodoptera frugiperda*: from genome-wide identification and developmental stage-related expression analysis to the perception of host plant odors, sex pheromones, and insecticides. Int. J. Mol. Sci. 24: 5595.

Jia, H.R, L.L. Niu, Y.F. Sun, Y.O. Liu and K.M. Wu. 2020. Odorant binding proteins and chemosensory proteins in *Episyrphus balteatus* (Diptera: Syrphidae): molecular cloning, expression profiling, and gene evolution. J. Insect Sci. 20(4). doi.org/10.1093/jisesa/ieaa065.

Li, M.Y., X.Y. Jiang, Y.Z. Qi, Y.J. Huang, S.G. Li and S. Liu. 2020. Identification and expression profiles of 14 odorant-binding protein genes from *Pieris rapae* (Lepidoptera: Pieridae). J. Insect Sci. 20(5): 2; 1–10.

Li, Y., L. Huien, Z.G. Wang, D.Y. Gao, K. Xiao and A.H. Yan. 2018. Cloning, localization and bioinformatics analysis of a gene encoding an odorant-binding protein (OBP) in *Anoplophora glabripennis* (Motschulsky). Invert. Neurosci. 18: 11.

Li, Z., J.J. Zhou, Z. Shen and L. Field. 2004. Identification and expression profiling of putative odorant-binding proteins in the malaria mosquitoes, *Anopheles gambiae* and *A. arabiensis*. Sci. China C Life Sci. 47: 567–576.

Liu, N.Y., K. Yang, Y. Liu, W. Xu, A. Anderson and S.L. Dong. 2015. Two general-odorant binding proteins in *Spodoptera litura* are differentially tuned to sex pheromones and plant odorants. Comp. Biochem. Physiol. Part A: Mol. Integr. Physiol. 180: 23–31.

Liu, S.X., D.Y. Xue, R. Cheng and H.X. Han. 2014. The complete mitogenome of *Apocheima cinerarius*, (Lepidoptera: Geometridae: Ennominae) and comparison with that of other lepidopteran insects. Gene 547: 136–144.

Livak, K.J. and T.D. Schmittgen. 2001. Analysis of relative gene expression data using real-time quantitative PCR and the 2(-delta delta CCT) method. Methods 25(4): 402–408.

Luo, J., Z. Zhang, D. Li, J. Liu, K. Li, X. Sun and L. He. 2021. Identification and functional analysis of *SlitOBP11* from *Spodoptera litura*. Front. Physiol. 12: 619816.

Ma, L. 2016. Molecular and functional characterization of chemosensory genes in *Ectropis oblique*. Chinese Academy of Agricultural Sciences, Beijing.

Millar, J.G., M. Giblin, D. Barton, D.A. Reynard, G.B. Neill and E.W. Underhill. 1990. Identification and field testing of female-produced sex pheromone components of the spring cankerworm, *Paleacrita vernata* Peck (Lepidoptera: Geometridae). J. Chem. Ecol. 16: 3393–3409.

Paula, D.P., R.C. Togawa, M.C. Costa, P. Grynberg, N.F. Martins and D.A. Andow. 2016. Identification and expression profile of odorant binding proteins in *Halyomorpha halys* (Hemiptera: Pentatomidae). Insect Mol. Biol. 25(5): 580–594.

Pelletier, J., and W.S. Leal. 2009. Genome analysis and expression patterns of odorant binding proteins from the southern house mosquito *Culex pipiens quinquefasciatus*. PLoS One 44(7): e6237.

Ribeiro, J.M., F.A. Genta, M.H. Sorgine, R. Logullo, R.D. Mesquita, G.O. Paiva-Silva, D. Majerowicz, M. Medeiros, L. Koerich, W.R. Terra, C. Ferreira, A.C. Pimentel, P.M. Bisch, D.C. Leite, M.M. Diniz, M.L. da Silva, R.N. Araujo, A.C. Gandara, S. Brosson, D. Salmon, S. Bousbata, N. González-Caballero, A.M. Silber, M. Alves-Bezerra, K.C. Gondim, M.A. Silva-Neto, G.C. Atella, H. Araujo, F.A. Dias, C. Polycarpo, R.J. Vionette-Amaral, P. Fampa, A.C. Melo, A.S. Tanaka, C. Balczun, J.H. Oliveira, R.L. Gonçalves, C. Lazoski, R. Rivera Pomar, L. Diambra, G.A. Schaub, E.S. Garcia, P. Azambuja, G.R. Braz and P.L. Oliveira. 2014. An insight into the transcriptome of the digestive tract of the bloodsucking bug. *Rhodnius prolixus*. PLoS Negl Trop Dis 8.

Si, P.F., Q. Zhou and Z.Y. Cui. 2018. Cloning, prokaryotic expression and tissue expression profiling of an odorant binding protein BminOBP25 from gene *Bactrocera minax* (Diptera: Tephritidae). Acta Entomol. Sinica 61(05): 537–545.

Song, Y.Q., Z.Y. Song, H.Z. Gu, H.Z. Sun and J.Y. Zhao. 2021. Identification and expression analysis of odorant-binding proteins and chemosensory proteins in the antennal transcriptome of *Yemma signatus* (Hsiao, 1974). Phytoparasitica 49(5): 917–933.

Su, C.Y., K. Menuz and J.R. Carlson. 2009. Olfactory perception: receptors, cells, and circuits. Cell 139(1): 45–59.

Swarup, S., T.L. Williams and R.R.H. Anholt. 2011. Functional dissection of odorant binding protein genes in *Drosophila melanogaster*. Genes, Brain, and Behavior 10(6): 648–657.

Tang, Q.F., C. Shen, Y. Zhang, Z.P. Yang, R.R. Han and J. Wang. 2019. Antennal transcriptome analysis of the maize weevil *Sitophilus zeamais*: Identification and tissue expression profiling of candidate odorant-binding protein genes. Arch. Insect Biochem. Physiol. 101: e21542.

Tian, Z. 2016. Study on *Cydia pomonella* pheromone binding proteins and screening of potentially active semiochemicals. Northwest Agriculture and Forestry University, Yangling.

Wang, J.Z., P. Gao, T. Jing and Y.Q. Luo. 2019. Characterization and expression profiling of odorant-binding proteins in *Anoplophora glabripennis* Motsch. Gene 693: 25–26.

Wang, J.Z., P. Hu, P. Gao, T. Jing and Y.Q. Luo. 2017. Antennal transcriptome analysis and expression profiles of olfactory genes in *Anoplophora chinensis*. Sci. Rep. 7(1): 15470.

Wang, Q., Y.J. Li, Q. Wang, L. Sun and Y.J. Zhang. 2022. The *Adelphocoris lineolatus* OBP4: support for evolutionary and functional diver-gene of a mirid pheromone-binding protein from that found in lepidopteran moths. Insect Sci. 29(1): 151–161.

Wang, R., F. Li, W. Zhang, X. Zhang, C. Qu, G. Tetreau, L. Sun, C. Luo and J. Zhou. 2017. Identification and expression profile analysis of odorant binding protein and chemosensory protein genes in *Bemisia tabaci* MED by head transcriptome. PLoS One 12: e0171739.

Yan, Y.T., F. Wu, Y.L. Zhang, X.B. Fu, H.C. Cui, B.Y. Han and H.L. Li. 2021. Study on the differences in ligand-binding function and mode of the antennal high-abundance odorant-binding proteins *EoblOBP9* and *EoblOBP11* of the tea geometrid, *Ectropis obliqua* Prout. J. Tea Sci. 41(05): 643–653.

Yang, Y.C., W.B. Li, J. Tao and S.X. Zong. 2019. Antennal transcriptome analy-ses and olfactory protein identification in an important wood-boring moth pest, *Streltzoviella insularis* (Lepidoptera: Cossidae). Sci. Rep. 9(1): 17951.

Zhang, F., A. Merchant, Z. Zhao, Y. Zhang, J. Zhang, Q. Zhang, Q. Wang, X. Zhou and X. Li. 2020. Characterization of *MaltOBP1*, a minus-C odorant-binding protein, from the Japanese pine sawyer beetle, *Monochamus alternatus* Hope (Coleoptera: Cerambycidae). Front. Physiol. 11: 212.

Zhang, S.H., Q.Q. Meng, A.Q. Liu, R.H. Yan, X.W. Lin, S.W. Sun, F.P. Li and Z. Wang. 2023. Cloning and tissue expression profiling of the odorant binding protein gene *HtheOBP3* in tea mosquito bug *Helopeltis theivora.* J. Plt. Prot. 50(01): 71–80.

Zhang, Y. N., J.Y. Jin, R. Jin, Y.H. Xia, J.J. Zhou, J.Y. Deng, S.L. Dong and R. Michel. 2013. Differential expression patterns in chemosensory and non-chemosensory tissues of putative chemosensory genes identified by transcriptome analysis of insect pest the purple stem borer *Sesamia inferens* (Walker). PLoS ONE 8(7): e69715.

Zhang, Z.K., Y. Zhang, S.Y. Wu and Z.R. Lei. 2017. Recent advances in odorant binding proteins of insects. J. Environ. Entomol. 39(03): 713–720.

Zhou, J.J. 2010. Odorant-binding proteins in insects. Vitamins and Hormones 83: 241–272.